

## 在纯水体系和活细胞中高选择检测 $\text{Fe}^{3+}$ 的香豆素荧光探针

刘琪梦 汪 欢 郭昊冉 郭 媛\*

(西北大学化学与材料科学学院, 国家级化学实验教育示范中心, 西安 710127)

**摘要:** 设计、合成了一种香豆素类荧光探针 **CF470**, 该探针通过引入高水溶性且选择性与  $\text{Fe}^{3+}$  配位的多羟基基团实现了纯水体系中  $\text{Fe}^{3+}$  的检测。当在探针体系中加入  $\text{Fe}^{3+}$  后, 其强烈的蓝色荧光在 2 min 内就可被完全猝灭。探针不仅对  $\text{Fe}^{3+}$  快速、高选择响应, 而且由于引入了亲水的多羟基基团具有良好的水溶性。更重要的是, 探针对活细胞低毒、生物相容性好, 被成功应用于活细胞中  $\text{Fe}^{3+}$  的成像。

**关键词:** 铁离子; 香豆素; 纯水体系; 荧光成像; 活细胞

中图分类号: O626.23 文献标识码: A 文章编号: 1001-4861(2019)05-0923-07

DOI: 10.11862/CJIC.2019.090

## A Highly Selective Coumarin-based Fluorescent Probe for Detecting $\text{Fe}^{3+}$ in Pure Water Systems and Living Cells

LIU Qi-Meng WANG Huan GUO Hao-Ran GUO Yuan\*

(National Demonstration Center for Experimental Chemistry Education,  
College of Chemistry and Materials Science, Northwest University, Xi'an 710127, China)

**Abstract:** A novel fluorescent probe **CF470** was designed and synthesized, for detecting  $\text{Fe}^{3+}$  in pure water systems, composed of coumarin derivative as a fluorophore, and the trihydroxyl group as both the  $\text{Fe}^{3+}$ -sensing site and hydrophilic group. Adding  $\text{Fe}^{3+}$  into the solution of **CF470** rendered intense blue fluorescence quenching within 2 min. The probe showed excellent specificity, outstanding water-solubility in virtue of presence of the exceedingly hydrophilic trihydroxyl moiety, and fast response time. More importantly, the low cytotoxic and good biocompatible probe was also successfully utilized to image  $\text{Fe}^{3+}$  in living cells.

**Keywords:** iron ions; coumarin; pure water systems; fluorescent imaging; living cells

Many heavy metal ions have attracted great attention owing to their broader influence on the environment and human health<sup>[1-2]</sup>. In particular, iron ( $\text{Fe}^{3+}$ ) is one of the most plentiful transition elements, and it performs crucial roles in many physiologic processes including cell metabolism, hemoglobin formation and so on<sup>[3-7]</sup>. However, abnormal  $\text{Fe}^{3+}$  content may cause many serious diseases to people, for

instance, abdominal pain, hyperferremic disorders, Parkinson's disease and Alzheimer's disease<sup>[8-10]</sup>. Thus, it is of considerable importance to develop an efficient method for highly selective detection of  $\text{Fe}^{3+}$ .

Compared with conventional analytical methods like colorimetry and voltammetry<sup>[11-14]</sup>, fluorescent probes have been regarded as one of the most valid tools to detect  $\text{Fe}^{3+}$  due to the advantages of simple

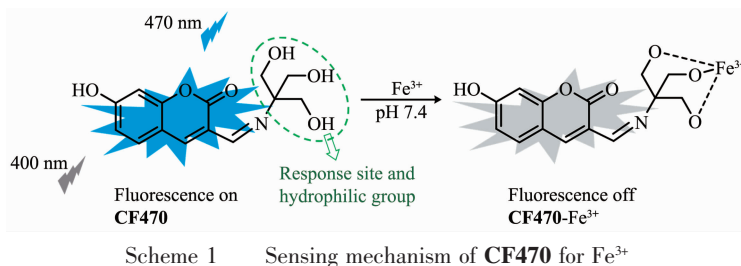
收稿日期: 2018-12-08。收修改稿日期: 2019-01-19。

国家自然科学基金(No.21472148, 21072158), 陕西高等教育精品课程建设基金和西北大学优秀青年学术骨干支持计划资助项目。

\*通信联系人。E-mail: guoyuan@nwnu.edu.cn

manipulation, high sensitivity and low cost<sup>[15-21]</sup>. Hence, an increasing number of  $\text{Fe}^{3+}$  fluorescent probes based on the different mechanisms have been developed<sup>[22-31]</sup>. Unfortunately, among these developed  $\text{Fe}^{3+}$  fluorescent probes, many fluorescent probes are easily interfered with  $\text{Al}^{3+}$ ,  $\text{Cu}^{2+}$  and  $\text{Cr}^{3+}$ , and few of probes possess ideal water-solubility. To the best of our knowledge, ideal water-solubility is conducive to the biological application of probes. Therefore, it is highly desired to develop a high selective fluorescent probe for detecting  $\text{Fe}^{3+}$  in 100% aqueous medium. We herein designed and synthesized a novel fluorescent probe **CF470** for sensing  $\text{Fe}^{3+}$  in deionized water. **CF470** was designed

by using coumarin derivative as a fluorophore, and the trihydroxyl group as both the response site and hydrophilic group, as shown in Scheme 1. The intense blue fluorescence of **CF470** was quenched within 2 min after the addition of  $\text{Fe}^{3+}$  (100 equiv.), which was attributed to the paramagnetic quenching effect. As expected, the probe **CF470** not only possessed good selectivity, ideal water-solubility owing to existence of the exceedingly hydrophilic trihydroxyl group, but also had a rapid response to  $\text{Fe}^{3+}$ . In especial, the probe, with low toxicity and good biocompatibility, was successfully employed to image  $\text{Fe}^{3+}$  in A549 cells.



## 1 Experimental

### 1.1 Materials and instruments

All materials, unless special stated, were obtained from commercial sources and used without further purification. Fluorescence spectra and absorption spectra were performed on a Hitachi F-2700 fluorescence spectrophotometer and Shimadzu UV-2550 spectrometer, respectively. For all spectral measurements, the excitation wavelength was set at 400 nm, and the slit widths of excitation and emission were 2.5 nm and 5 nm, respectively. NMR spectra were obtained on a Varian Unity INOVA-400 spectrometer with tetramethylsilane (TMS) as an internal standard. A Mettler Toledo pH meter was used for the all pH measurements. High-resolution mass spectra were measured on a Bruker micrOTOF-Q II mass spectrometer. Infrared spectra were acquired with a Bruker Vertex 70 FI-IR spectrometer. The cell experiments were carried out with an Olympus FV1000 confocal microscope.

### 1.2 Preparation of sample solutions

For all spectrometric studies, **CF470** was

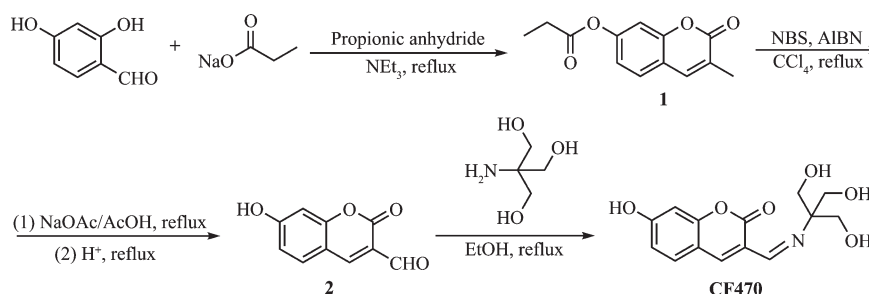
prepared in analytical grade DMSO to obtain the stock solution of the probe ( $1 \text{ mmol} \cdot \text{L}^{-1}$ ). Stock solutions of various metal ions, such as  $\text{Fe}^{3+}$ ,  $\text{Fe}^{2+}$ ,  $\text{K}^+$ ,  $\text{Mn}^{2+}$ ,  $\text{Ni}^{2+}$ ,  $\text{Cd}^{2+}$ ,  $\text{Al}^{3+}$ ,  $\text{Co}^{2+}$ ,  $\text{Cr}^{3+}$ ,  $\text{Mg}^{2+}$ ,  $\text{Hg}^{2+}$ ,  $\text{Ba}^{2+}$ ,  $\text{Zn}^{2+}$ ,  $\text{Cu}^{2+}$ ,  $\text{Ca}^{2+}$ ,  $\text{Pb}^{2+}$ ,  $\text{Na}^+$ ,  $\text{Sn}^{2+}$ , and  $\text{Ag}^+$  were prepared in doubly distilled water ( $10 \text{ mmol} \cdot \text{L}^{-1}$ , respectively).

### 1.3 Synthesis of probe CF470

Synthesis of **CF470** was presented in Scheme 2. The characterization details were displayed in the supporting information (Fig.S3~S10).

#### 1.3.1 Synthesis of compound 1

A mixture of 2,4-dihydroxybenzaldehyde (0.69 g, 5.0 mmol), three drops of triethylamine and anhydrous sodium acetate (1.05 g, 11.0 mmol) in propionic anhydride (15 mL) was stirred at  $140^\circ\text{C}$  for 6 h. After 6 h, 100 mL ice-water was poured onto the mixture solution. Then the solution was removed by filtration, and the residue was recrystallized from methanol to obtain white solid. Yield: 56%.  $^1\text{H}$  NMR (400 MHz,  $\text{CDCl}_3$ )  $\delta$ : 7.54 (s, 1H), 7.45 (d,  $J=8.0$  Hz, 1H), 7.12 (s, 1H), 7.05 (d,  $J=8.0$  Hz, 1H), 2.70~2.64 (m, 2H), 2.24 (s, 3H), 1.31 (t,  $J=6.0$  Hz, 3H). HRMS:  $m/z$  Calcd. for  $\text{C}_{13}\text{H}_{13}\text{O}_4^+$  [ $\text{M}+\text{H}$ ] $^+$ : 233.079 5, Found: 233.080 8.

Scheme 2 Synthetic route of **CF470**

### 1.3.2 Synthesis of compound **2**

A mixture of compound **1** (1.16 g, 5.0 mmol), NBS (2.23 g, 12.5 mmol) and a trace amount of AIBN was dissolved in  $\text{CCl}_4$  (150 mL). After the mixture was stirred at 80 °C for 12 h, the solvent was evaporated under reduced pressure to give the resulting residue. The mixture of the resulting residue, sodium acetate (2.42 g, 29.5 mmol) and acetic acid (80 mL) was unceasingly stirred at 100 °C for 12 h. HCl (2 mol·L<sup>-1</sup>, 80 mL) was poured in the mixture solution and unceasingly stirred for 30 min. The solution then was cooled down to room temperature and was discarded by filtration. The resulting crude solid was washed with water (10 mL) and methanol (10 mL) to afford brown powder. (870 mg, 87%). <sup>1</sup>H NMR (400 MHz, DMSO-*d*<sub>6</sub>)  $\delta$ : 11.30 (s, 1H), 9.96 (s, 1H), 8.58 (s, 1H), 7.82(d, *J*=12.0 Hz, 1H), 6.87 (d, *J*=8.0 Hz, 1H), 6.77 (s, 1H). HRMS: *m/z* Calcd. for  $\text{C}_{10}\text{H}_7\text{O}_4^+$  [M+H]<sup>+</sup>: 191.019 8, Found: 191.018 6.

### 1.3.3 Synthesis of probe **CF470**

A mixture of compound **2** (190 mg, 1.0 mmol) and tris (hydroxymethyl) aminomethane (145.2 mg, 1.2 mmol) in ethanol (5 mL) was refluxed at 80 °C under the argon atmosphere. After the reaction completed, the solution was cooled to room temperature, the precipitate was acquired through filtration, washed with anhydrous ethanol to obtain orange product (100 mg, 75%). <sup>1</sup>H NMR (400 MHz, DMSO-*d*<sub>6</sub>)  $\delta$ : 10.60 (s, 1H), 8.05 (s, 1H), 7.60 (d, *J*=8.0 Hz, 1H), 6.79 (d, *J*=8.0 Hz, 1H), 6.72 (s, 1H), 5.35 (s, 1H), 4.75 (s, 1H), 3.70 (d, *J*=8.0 Hz, 1H), 3.62 (s, *J*=8.0 Hz, 1H), 3.41 (s, 4H). <sup>13</sup>C NMR (100 MHz, DMSO-*d*<sub>6</sub>)  $\delta$ : 162.03, 160.27, 155.43, 140.69, 130.58, 122.38, 113.83, 111.40, 102.31, 87.70, 69.27, 67.48, 63.11, 62.69. HRMS: *m/z* Calcd.

for  $\text{C}_{14}\text{H}_{16}\text{NO}_6^+$  [M+H]<sup>+</sup>: 294.095 9, Found: 294.097 2. IR (KBr, cm<sup>-1</sup>)  $\nu$ : 3 296, 2 801, 1 698, 1 616, 1 361, 1 250, 1 191, 1 114, 864, 764, 655, 505.

## 1.4 Detection limit

The detection limit of **CF470** for detecting  $\text{Fe}^{3+}$  was calculated by means of following equation:

$$\text{Detection limit} = 3\sigma/k$$

$\sigma$  is the standard deviation of eleven blank measurements and *k* is the slope of standard curve.

## 1.5 Cytotoxicity assay

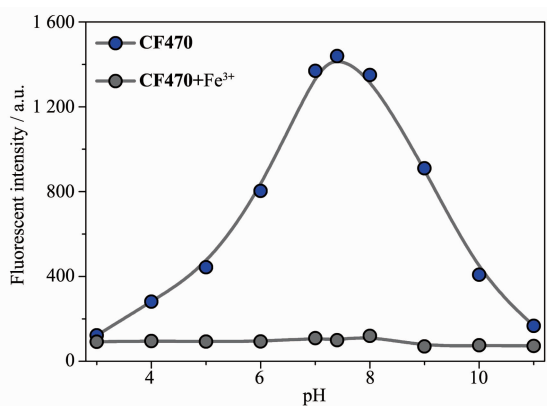
Cytotoxicity studies of **CF470** to A549 cells were evaluated using standard MTT assay. Cells were incubated in 96-well microplates at a density of  $1 \times 10^5$  cells per well in Dulbecco's modified Eagle's medium (DMEM) containing 10% fetal calf serum for 24 h. After that, different concentrations of **CF470** (0, 5, 10, 15, 20 and 25  $\mu\text{mol} \cdot \text{L}^{-1}$ ) were added the culture dish and treated for 24 h. MTT reagent (10  $\mu\text{L}$ ) was added and sequentially incubated for 4 h. Then, the culture medium was washed with PBS three times and DMSO (200  $\mu\text{L}$ ) was cultured with cells to dissolve formazan. The absorbance at 490 nm was recorded using the microplate reader.

# 2 Results and discussion

## 2.1 Spectral properties of probe **CF470**

In consideration of the effect of pH on the properties of the fluorescent probe, we initially examined the fluorescence intensities of the probe and reaction product within various pH values (3.0~11.0). Fig.1 showed that the probe **CF470** exhibited a maximum fluorescence emission intensity at 470 nm and the fluorescence intensity was almost stable with pH ranging from 7.0 to 8.0. After adding hundred

equivalences of  $\text{Fe}^{3+}$ , fluorescence intensity at 470 nm of **CF470** was drastically weakened and kept fine stability within a wide pH region of 3.0~11.0. Given the cell imaging and spectral response of **CF470** to  $\text{Fe}^{3+}$ , all experiments selected pH 7.4.



$\lambda_{\text{ex}}=400$  nm,  $\lambda_{\text{em}}=470$  nm, slit: 2.5 nm/5 nm

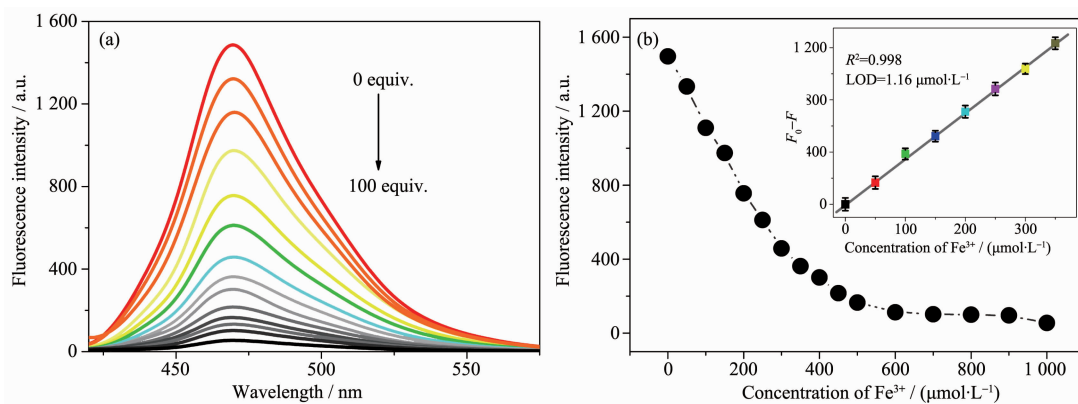
Fig.1 Fluorescence intensity at 470 nm of **CF470** ( $10 \mu\text{mol}\cdot\text{L}^{-1}$ ) before and after adding  $\text{Fe}^{3+}$  (100 equiv.) at different pH values

UV-Vis absorption spectra of **CF470** toward  $\text{Fe}^{3+}$  was firstly studied in phosphate buffer (pH=7.4) solution (Fig.S1). The free **CF470** exhibited a main absorption peak at 410 nm. With successive addition of  $\text{Fe}^{3+}$  (0~100 equiv.) into the buffer solution of **CF470**, the absorption peak at 410 nm gradually enhanced. We also estimated the fluorescence spectra of **CF470** to  $\text{Fe}^{3+}$  (Fig.2a). The probe **CF470** displayed a strong blue fluorescence. However, upon the addition of  $\text{Fe}^{3+}$

(0~100 equiv.) to **CF470** solution, a significant fluorescence attenuation was observed, which was attributed to the paramagnetic quenching effect. After the reaction between probe and  $\text{Fe}^{3+}$  (100 equiv.), the strong fluorescence almost entirely disappeared (Fig.2b). And the fluorescence intensity at 470 nm demonstrated good linear relationship with the concentrations of  $\text{Fe}^{3+}$  (0~35 equiv.) with a detection limit ( $1.16 \mu\text{mol}\cdot\text{L}^{-1}$ ) ( $S/N=3$ ) (Fig.2b inset). The results showed that **CF470** could realize quantitative detection of  $\text{Fe}^{3+}$ .

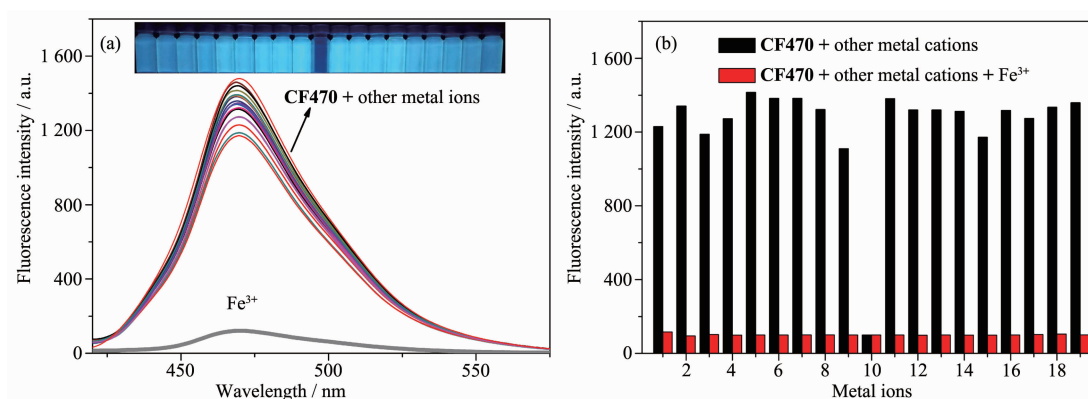
To study the selectivity of **CF470** toward  $\text{Fe}^{3+}$ , different metal ions were examined under same conditions (Fig.3a). **CF470** demonstrated obvious fluorescence quenching in the presence of  $\text{Fe}^{3+}$  in phosphate buffer (pH=7.4) solution, while other metal ions did not cause significant fluorescence attenuation and color changes on **CF470** than  $\text{Fe}^{3+}$  (Fig.3a inset). Simultaneously, competition experiments were also conducted (Fig.3b). When  $\text{Fe}^{3+}$  (100 equiv.) was added to the mixture solution of **CF470** and other metal ions, a clear fluorescence attenuation was discerned, indicating that the presence of other metal ions could not interfere **CF470** for detecting  $\text{Fe}^{3+}$ . Thus, the above experimental results demonstrated that **CF470** had high specificity for  $\text{Fe}^{3+}$ .

To assess the response ability of **CF470** for  $\text{Fe}^{3+}$ , the kinetic studies were carried out (Fig.4a). The addition of  $\text{Fe}^{3+}$  (100 equiv.) to the solution of **CF470**



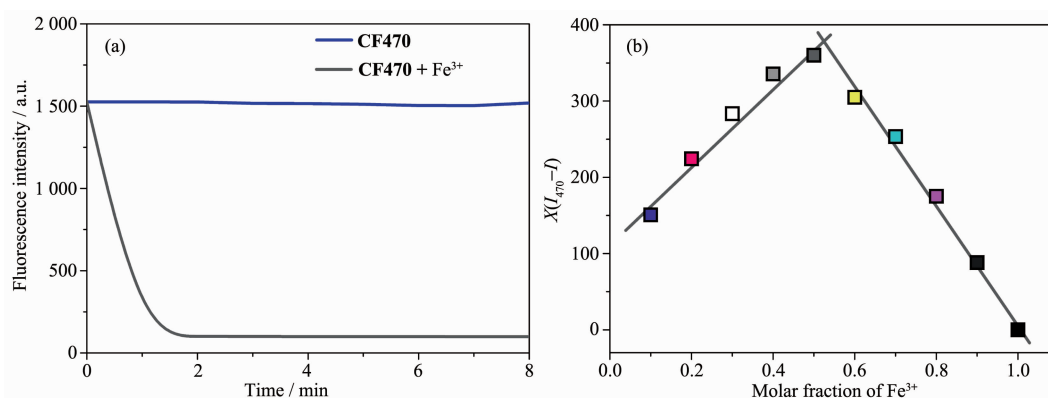
Inset: the linear correlation between fluorescence intensity at 470 nm of **CF470** ( $10 \mu\text{mol}\cdot\text{L}^{-1}$ ) and  $\text{Fe}^{3+}$  concentrations (0~35 equiv.) in phosphate buffer (pH=7.4) solution ( $\lambda_{\text{ex}}=400$  nm,  $\lambda_{\text{em}}=470$  nm, slit: 2.5 nm/5 nm)

Fig.2 (a) Fluorescence spectra of **CF470** ( $10 \mu\text{mol}\cdot\text{L}^{-1}$ ) after adding different amounts of  $\text{Fe}^{3+}$  (0~100 equiv.); (b) Fluorescence intensity changes of **CF470** ( $10 \mu\text{mol}\cdot\text{L}^{-1}$ ) toward different concentrations of  $\text{Fe}^{3+}$  (0~100 equiv.) in phosphate buffer (pH=7.4) solution



1.  $\text{Ca}^{2+}$ , 2.  $\text{Ni}^{2+}$ , 3.  $\text{Zn}^{2+}$ , 4.  $\text{Pb}^{2+}$ , 5.  $\text{Cd}^{2+}$ , 6.  $\text{Cu}^{2+}$ , 7.  $\text{Sn}^{2+}$ , 8.  $\text{Ag}^+$ , 9.  $\text{Mg}^{2+}$ , 10.  $\text{Fe}^{3+}$ , 11.  $\text{K}^+$ , 12.  $\text{Na}^+$ , 13.  $\text{Fe}^{2+}$ , 14.  $\text{Cr}^{3+}$ , 15.  $\text{Ba}^{2+}$ , 16.  $\text{Mn}^{2+}$ , 17.  $\text{Co}^{2+}$ , 18.  $\text{Hg}^{2+}$ , 19.  $\text{Al}^{3+}$ ;  $\lambda_{\text{ex}}=400$  nm,  $\lambda_{\text{em}}=470$  nm, slit: 2.5 nm/5 nm

Fig.3 (a) Fluorescence responses of **CF470** ( $10 \mu\text{mol}\cdot\text{L}^{-1}$ ) to different metal ions (100 equiv.); Inset: photos of **CF470** ( $10 \mu\text{mol}\cdot\text{L}^{-1}$ ) after the addition of different metal ions (100 equiv.) under a handheld 365 nm UV lamp; (b) Fluorescence responses of **CF470** ( $10 \mu\text{mol}\cdot\text{L}^{-1}$ ) to  $\text{Fe}^{3+}$  (100 equiv.) in presence of different metal ions in phosphate buffer (pH=7.4) solution



Total concentration of **CF470** and  $\text{Fe}^{3+}$  was  $10 \mu\text{mol}\cdot\text{L}^{-1}$ , and  $X$  represented molar fraction of  $\text{Fe}^{3+}$  ( $\lambda_{\text{ex}}=400$  nm,  $\lambda_{\text{em}}=470$  nm, slit: 2.5 nm/5 nm)

Fig.4 (a) Plot of fluorescence intensity at 470 nm versus time for the reaction between **CF470** ( $10 \mu\text{mol}\cdot\text{L}^{-1}$ ) and  $\text{Fe}^{3+}$  (100 equiv.); (b) Job's plot of **CF470** in phosphate buffer (pH=7.4) solution

led to a remarkable attenuation in the fluorescence intensity at 470 nm, and the fluorescence intensity attained stable within 2 min, with a 25-fold decrease.

## 2.2 Proposed sensing mechanism

The possible sensing mechanism of **CF470** to  $\text{Fe}^{3+}$  was depicted in Scheme 1. The complexation of **CF470** with  $\text{Fe}^{3+}$  resulted in the fluorescence quenching, which was possibly ascribed to the paramagnetic property of  $\text{Fe}^{3+}$ . HRMS analysis and Job's plot were carried out to verify this mechanism. As depicted in Fig.4b, a strong fluorescence intensity at mole fraction 0.5 suggested 1:1 stoichiometry for the **CF470**- $\text{Fe}^{3+}$  complex. Similarly, the binding mode of **CF470** with  $\text{Fe}^{3+}$  was also testified by HRMS. After the probe

reacted with  $\text{Fe}^{3+}$ , a new peak at  $m/z=345.9987$  corresponding to  $[\text{CF470-Fe}^{3+}]$  appeared (Fig.S2). As a result, the experimental results fully confirmed the response mechanism of **CF470** toward  $\text{Fe}^{3+}$ .

## 2.3 Computational studies

To further prove the sensing mechanism of **CF470** toward  $\text{Fe}^{3+}$ , theoretical calculation was carried out by the Gaussian 09 program. The optimum structure and electron distributions of **CF470-Fe}^{3+} were obtained using B3LYP/6-31G(d,p) (Fig.5). The electrons on the HOMO of **CF470-Fe}^{3+} were mostly situated on coumarin moiety, whereas the electrons on the LUMO were mainly located around  $\text{Fe}^{3+}$ , suggesting that the fluorescence quenching was due to the coordination of****



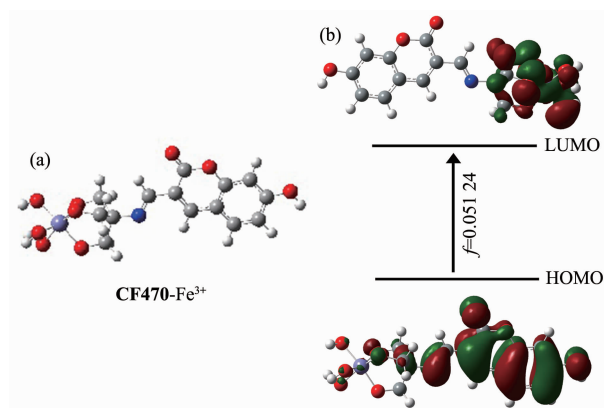


Fig.5 (a) Optimum structure and (b) HOMO-LUMO energy level of **CF470-Fe<sup>3+</sup>**

**CF470** with **Fe<sup>3+</sup>**.

## 2.4 Cellular imaging

To assess the toxicity of **CF470** (0, 5, 10, 15, 20 and 25  $\mu\text{mol}\cdot\text{L}^{-1}$ ) towards A549 cells, MTT assay was carried out. As shown in Fig.6, even after cells were cultured with high concentration of **CF470** (25  $\mu\text{mol}\cdot\text{L}^{-1}$ ) for 24 h, cell survival rate was still more than 80%, showing the low cytotoxicity and good biocompatibility of **CF470** to living cells.

Then, the cellular imaging experiments of **CF470** toward **Fe<sup>3+</sup>** were conducted on A549 cells. The A549

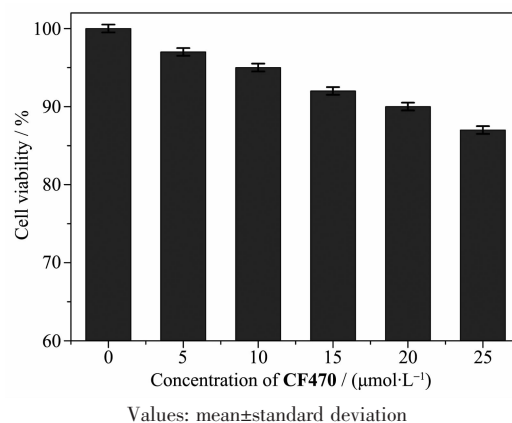


Fig.6 Cytotoxicity of **CF470** in A549 cells estimated by the MTT method

cells were cultured with **CF470** (10  $\mu\text{mol}\cdot\text{L}^{-1}$ ) in DMEM for 20 min. After that, cells were washed repeatedly with PBS for three times, and finally cultured with **Fe<sup>3+</sup>** (100 equiv.) for 10 min. As seen in Fig.7, strong blue fluorescence was observed after A549 cells was pretreated with **CF470**. In contrast, cells displayed slight fluorescence in the presence of **Fe<sup>3+</sup>**. These experimental results manifested that **CF470** possessed good cell membrane permeable as well as could be used for the detection of **Fe<sup>3+</sup>** in living cells.

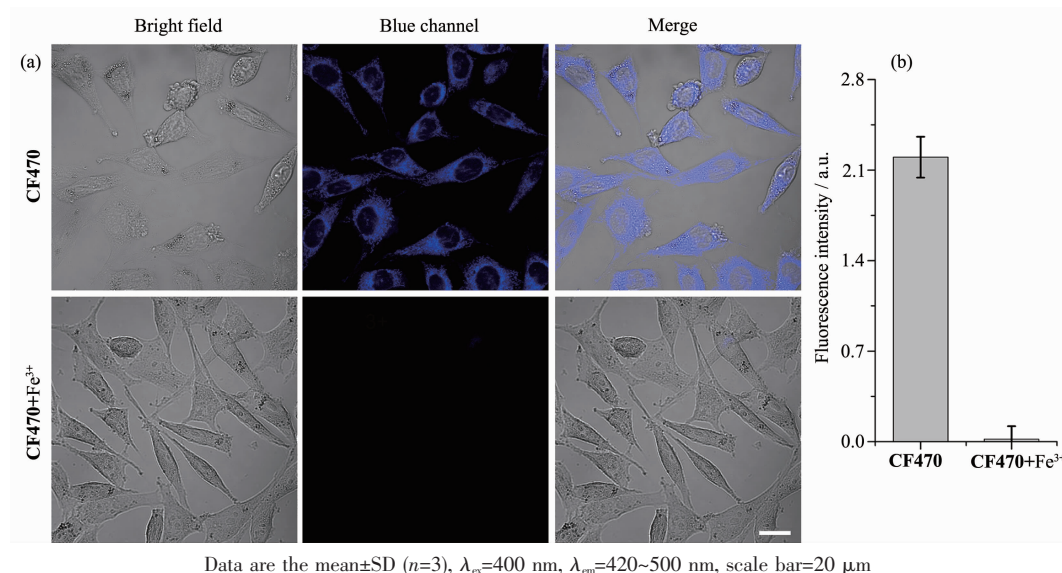


Fig.7 Cellular imaging of **Fe<sup>3+</sup>** in A549 cells cultured with **CF470** (10  $\mu\text{mol}\cdot\text{L}^{-1}$ , 20 min) and further incubated with **Fe<sup>3+</sup>** (1 000  $\mu\text{mol}\cdot\text{L}^{-1}$ , 10 min); (b) Fluorescence intensity per one blue channel

## 3 Conclusions

In summary, we have developed a novel fluorescent probe **CF470**, for detecting **Fe<sup>3+</sup>** in 100%

aqueous solution through complexation reaction on the basis of fluorescence quenching, comprised of coumarin derivative as a fluorophore, and the trihydroxyl group

as both the  $\text{Fe}^{3+}$ -sensing site and hydrophilic group. Remarkably, the sensing mechanism of **CF470** to  $\text{Fe}^{3+}$  was proved by HRMS analysis and theoretical calculation. A palpable fluorescence quenching was observed after the addition of  $\text{Fe}^{3+}$  into the **CF470** solution. The probe **CF470**, with ideal water-solubility on account of existence of the exceedingly hydrophilic trihydroxyl group, can realize a highly selective and rapid detection of  $\text{Fe}^{3+}$ . Furthermore, cell imaging results demonstrated that **CF470** with low cytotoxicity had admirable membrane permeability and could detect  $\text{Fe}^{3+}$  in living cells.

Supporting information is available at <http://www.wjhxsb.cn>

## References:

- [1] Wang H, Shi D L, Li J, et al. *Sens. Actuators B*, **2018**,**256**: 600-608
- [2] Dean K M, Qin Y, Palmer A E. *Biochim. Biophys. Acta*, **2012**,**1823**:1406-1415
- [3] Chen X, Pradhan T, Wang F, et al. *Chem. Rev.*, **2012**,**112**: 1910-1956
- [4] Du J, Hu M, Fan J, et al. *Chem. Soc. Rev.*, **2012**,**41**:4511-4535
- [5] Papanikolaou G, Pantopoulos K. *Toxicol. Appl. Pharmacol.*, **2005**,**202**:199-211
- [6] Andjelkovi M, Camp J V, Meulenaer B D, et al. *Food Chemistry*, **2006**,**98**:23-31
- [7] Hentze M W, Muckenthaler M U, Galy B, et al. *Cell*, **2010**, **142**:24-38
- [8] Zhao N, Sun Z, Mao Y, et al. *Cell. Physiol. Biochem.*, **2010**, **25**:587-594
- [9] Sui B, Tang S, Liu T, et al. *ACS Appl. Mater. Interfaces*, **2014**,**6**:18408-18412
- [10] ZHANG Yong(张勇), WANG Ji-Meng(王继猛), SHU Wei-Hu(舒威虎), et al. *Chinese J. Inorg. Chem.*(无机化学学报), **2013**,**29**:150-154
- [11] Meng W F, Yang M P, Li B, et al. *Tetrahedron*, **2014**,**70**: 8577-8581
- [12] CHEN Bang(陈邦), WANG Shao-Jing(王少静), Song Zhan-Ke(宋战科), et al. *Chinese J. Inorg. Chem.*(无机化学学报), **2017**,**33**:1722-1730
- [13] Zheng M, Tan H, Xie Z, et al. *ACS Appl. Mater. Interfaces*, **2013**,**5**:1078-1083
- [14] Cerchiaro G, Manieri T M, Bertuchi F R. *Metallomics*, **2013**, **5**:1336-1345
- [15] JIAO Yuan-Hong(焦元红), ZHANG Qian(张前), JIANG Yu-Feng(姜玉凤), et al. *Chinese J. Inorg. Chem.*(无机化学学报), **2015**,**31**:361-368
- [16] Wu J, Ye Z, Wu F, et al. *Talanta*, **2018**,**181**:239-247
- [17] Wang H, Yang D, Tan R, et al. *Sens. Actuators B*, **2017**,**247**: 883-888
- [18] En D, Guo Y, Chen B T, et al. *RSC Adv.*, **2014**,**4**:248-253
- [19] Wu X, Niu Q, Li T. *Sens. Actuators B*, **2016**,**222**:714-720
- [20] Yang X H, Li S, Tang Z S, et al. *Chin. Chem. Lett.*, **2015**, **26**:129-132
- [21] Yan L, Yang M, Leng X, et al. *Tetrahedron*, **2016**,**72**:4361-4367
- [22] Joshi S, Kumari S, Bhattacharjee R, et al. *Sens. Actuators B*, **2015**,**220**:1266-1278
- [23] Pathak S, Das D, Kundu A, et al. *RSC Adv.*, **2015**,**5**:17308-17318
- [24] Maity S, Kundu A, Pramanik A. *RSC Adv.*, **2015**,**5**:52852-52865
- [25] Cherreddy N R, Thennarasu S, Mandal A B. *Analyst*, **2013**, **138**:1334-1337
- [26] Saleem M, Abdullah R, Ali A, et al. *Bioorg. Med. Chem.*, **2014**,**22**:2045-2051
- [27] Xie P, Guo F, Xia R, et al. *J. Lumin.*, **2014**,**145**:849-854
- [28] Zhou X, Wu X, Yoon J. *Chem. Commun.*, **2015**,**51**:111-113
- [29] Wang K P, Lei Y, Zhang S J, et al. *Sens. Actuators B*, **2017**,**225**:1140-1145
- [30] Wang Y, Song F, Zhu J, et al. *Tetrahedron Lett.*, **2018**,**59**: 3756-3762
- [31] Wang C, Liu Y, Cheng J, et al. *J. Lumin.*, **2015**,**157**:143-148